ISSN: 2639-7536

Review Article

Petroleum and Chemical Industry International

A Three-Dimensional Thermo-hydrodynamic Simulation of Compact Cross-Flow Plate Heat Exchanger

Yahya Sheikhnejad*, Jorge Ferreira, Nelson Martins

Centre for Mechanical Technology and Automation, Department of Mechanical Engineering, University of Aveiro

***Corresponding author**
Yahya Sheikhnejad, Department of Mechanical Engineering, University of Avairo, Campus U. de Santiago, 3810-193, Aveiro, Portugal, E-mail: yahya@ua.pt

Submitted: 06 Nov 2018; **Accepted**: 22 Nov 2018; **Published**: 08 Jan 2019

Abstract

This study is dedicated to the thermal analysis and thermo-hydrodynamic simulation of an air-to-air plate heat exchanger in order to solve its routine problem in industry. The compact type of cross-flow plate heat exchanger, in which corrugated plates pile up tightly and delicately brazed to each other, has been used in many situations and has many applications from food industries to petroleum and military. Routinely, after a certain lifespan, the brazed joints are detached and cause a mixture of hot and cold fluids as well as highly reduction of heat exchanger performance. This problem leads to increase the system maintenance significantly. Apart from the imposed cost and time for its maintenance, which is indeed a crucial problem? Finally, to have a better understanding, a three-dimensional numerical investigation on thermo-hydrodynamic analysis of conjugate heat transfer was performed using computational fluid dynamics techniques. Forced convection heat transfer for fluid flow and conduction through solid material were considered as well. For simulation of steady state flow of Newtonian fluid, the governing equation was discredited by finite volume method and solved by the semi-implicit method for the pressure-linked equation. It was also found that both temperature and temperature gradient play an important role in this problem.

Keywords: Compact plate heat exchanger, thermal simulation, CFD, conjugate heat transfer.

Introduction

Engineering always comes up with solution of a real problem and facilitate a procedure using fundamental physics laws as well as crafty innovation. Hundreds of scientific papers about the heat transfer clearly have proven that, this concept has been the constant inevitable problem in different area over the time. Researchers also have suggested different methodologies [1-4]. The heat exchangers are stereotype facilities that have been a source of many challenges in this way. Still, they are challenging technology and call for more innovation and better performance [5]. Day by day, due to the limitation on energy consumption and operational dimension, heat exchanger design have been oriented to higher performance and smaller size and exploitation of nano fluid as well [6-12].

All cross-flow compact heat exchangers, especially those that have been designed and constructed for aviation industries, have a vital task as they are integrated into the whole system. Mainly their output is a thermally tuned fluid with a mission to keep the precious expensive instruments in a safe thermal zone. Any malfunction or deviation from their normal performance yield to loss the whole system and waste many resources from money to time. Practically, for the aviation industries applications, it results in losing that airplane while it is essential to be used. Numerical analysis and simulation of these compact plate heat exchangers have been presented in recent studies [13, 15].

Now by considering a typical air-to-air compact cross-flow plate heat exchanger which has some corrugated plates brazed to each other such that direction of grooves for two successive plates is perpendicular. Moreover, depending of the designer attitude, grooves can be in common rectangular or triangular form. This type of heat exchanger due to its high thermal performance relative to its size is popular and has been used in many industries. It means that it can be exposed of any thermal and hydrodynamic boundary condition. To determine its boundary conditions, it is needed to consider one of its applications in industry.

Here, it is consider plate heat exchanger application in avionics. Consequently, the information about the hot and cold sides should be extracted from the standard operation condition. With these explanations, the hot exhaust air from the 17th stage of compressor in high temperature and pressure guided through air-to-air heat exchanger and then conducted to cooling turbine. Usually speed of most of airplanes is between 700 to 900 km/h under no rush or harsh situation. In addition, its altitude varies between 20,000 to 30,000 feet depending on its mission and topography of its path.

In this study, the core of avionics heat exchanger is used for equipment heating and to protect them from frizzing. It is categorized into plate

heat exchanger division and supposed to take high temperature product of combustion near 700 K from the 17th row of compressor in order to warm up the cold fresh air at almost 250 K from ambient at 20000 feet, in order to deliver it to avionics equipment in moderate temperature.

According to the specification of jet engine, hot product of combustion with 500 m/s at 800 K and 19000 kPa is conducted toward heat exchanger through the short pipe. According to and knowing the flight altitude, characteristics of cold air namely temperature, pressure and density, can be extracted [16-18]. The thermodynamic properties of hot and cold entrance are provided in table 1.

Table 1: Thermos-physical properties of hot and cold air at the entrance of heat exchanger

Property	Cold	Hot
Pressure	42 kPa	19000 kPa (190 bar)
Temperature	250 K	700 K (800 F)
Velocity	700 km/h	548.64km/h (500 ft/s)
Viscosity	1.488×10^{-5} kg/m.s	3.332×10^{-5} kg/m.s
Density	0.64 kg/m^3	6.177 kg/m^3

Problem Statement

The main problem that frequently occurs in the cross-flow plate heat exchanger is the corruption and detachment of brazed corrugated plates that causes hot and cold mixture and reduction of heat exchanger performance. The detachment of plates create longitudinal cracks in plates and different pressure values in hot and cold sides leads to a leakage from higher pressure to lower pressure region. In fact, due to the high-pressure condition, usually in hot side, considerable flow rate would be lost due to the detachment problem. Hence, small amount of warm fluid has not this ability to keep avionics in a safe thermal condition and electronic equipment freezing very likely to happen.

The first problem that have to be solved is the determination of flow regime through the rectangular and triangular channels, Fig. 1(a). The criteria that is used as an indicator to have a good estimation of flow regime is the non-dimensional Reynolds number $\left(\frac{\rho \bar{V} D_h}{\eta_{air}}\right)$.

Hence, the only unknown parameter for calculation of Reynolds number is the flow rate. Also, to calculate a flow rate it is required to integrate velocity profile over cross section area of a channel. However, there is a closed-form analytical solution for the velocity profile only for the fully developed region. The entrance length, after which there is fully developed flow through the channel is proportional to the channel hydraulic diameter, $D_h = \frac{4A}{P}$ where A and P are the wet cross section area and wet perimeter in the channel. Due to the small hydraulic diameter, Fig. 2, for both hot and cold channels, Fig. 1(b & c), with a good approximation it can be concluded that only a small part of channel is in entrance length almost whole channel experience fully developed flow.

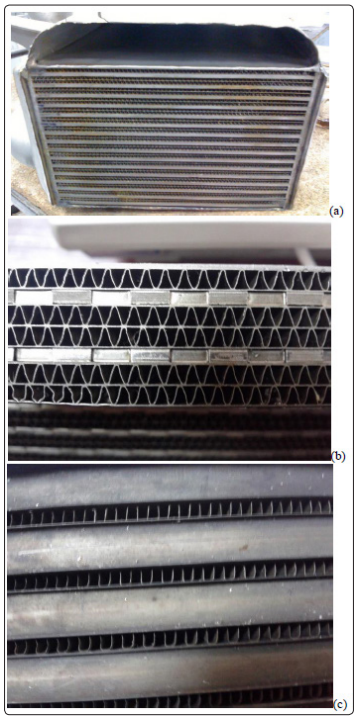

Figure 1: (a): Photo of inlet cold air of heat exchanger, (b): Zoomed photo on triangular channels for the cold air. (c): Semi-rectangular U-shaped channels for hot fluid.

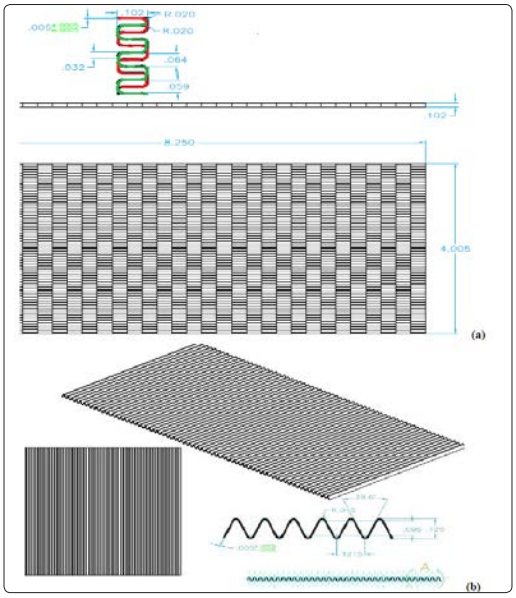

Figure 2: (a): Dimensions and configuration of semi-rectangular channels, (b): Dimensions and configuration of triangular channels.

The fully developed flow formula for velocity profile and flow rate through triangular and rectangular channel were presented by White [19]:

$$Q_t = \frac{a^4\sqrt{3}}{320\,\mu}\left(-\frac{\partial P}{\partial x}\right) \quad (1)$$

$$Q_r = \frac{4ba^3}{3\mu}\left(-\frac{\partial P}{\partial x}\right)\left[1-\frac{192a}{b\pi^5}\sum_{i=1,3,5,\ldots}^{\infty}\frac{\tanh\left(\frac{i\pi b}{2a}\right)}{i^5}\right] \quad (2)$$

Where t and r are corresponding to the triangle and rectangle words respectively. Also, geometrical parameters in Eq. (1) and (2) are presented in Fig. 3 and given in table 1 and 2.

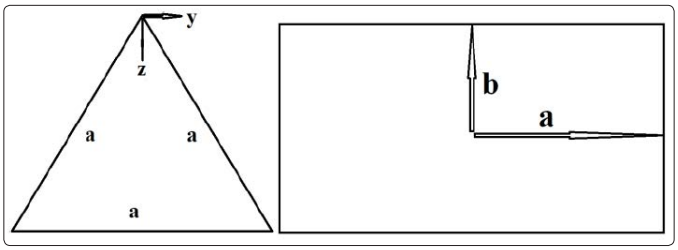

Figure 3: Parameters of triangular and rectangular channels

Table 2: Geometrical dimensions and flow conditions for triangular and rectangular channels

	a	b	L	P_2
Triangular channel	0.130 in	--	0.222 m	101.3 kPa
Rectangular channel	100.5 mm	12.5 mm	0.222 m	101.3 kPa

By considering this fact that in fully developed region we have $\left(\frac{\partial P}{\partial x}\right)=\frac{\Delta P}{L}$, $\Delta P = P_2 - P_1$, and then by substituting the value of parameters into Eq. (1) and (2) they yield into Eqs. (3) to (5).

$$\frac{(\Delta P)_t}{\rho} = 340 Q_t \quad (3)$$

$$\frac{(\Delta P)_r}{\rho} = 0.008 Q_r \quad (4)$$

$$Q = (N_t Q_t) + Q_r \quad (5)$$

Where NT=2×16×130=4160, total flow rate of cold air is Q=2.56 m^3/s. For the Eqs. (3) to (5) there is an analytic closed form solution as follows:

$$Q_r = \frac{\frac{C_t}{N_t}Q - (\Delta P_2/\rho)}{\frac{C_t}{N_t}+C_r} \quad (6)$$

$$Q_t = \frac{C_r Q + (\Delta P_2/\rho)}{C_t + C_r N_t} \quad (7)$$

$$\Delta P_2 = P_{2r} - P_{2t} \quad (8)$$

Where the constants are C_r =0.008, C_t =340. Equations (6-8) show that when there is outlet pressure for both channels then shared flow rates are only depending on the geometry of channels. After substituting the corresponding values, table 3 gives the unknown values.

Table 3: Hydraulic parameters of triangle and rectangle channels

$Q_t\,(m^3/s)$	$Q_r\,(m^3/s)$	$\Delta P_t\,(KPa)$	$\Delta P_r\,(KPa)$
54.865×10^{-6}	2.3317	0.012	0.012

While Reynolds number requires averaged velocity, simply by dividing the obtained flow rate to the channels cross section area, it can be calculated. The thermo-hydrodynamic characteristics of hot and cold channels are presented in table 4.

Table 4: thermo-hydrodynamic characteristics of hot and cold channels

	Hot channel	Cold channel
Reynolds number (Re)	2190	809
Peclet number (Pe)	1498	582
Prandtle number (Pr)	0.684	0.720

According to the obtained Reynolds number, it can be concluded that both hot and cold channels are in laminar regime.

In the modelling of 3D geometry of heat exchanger, in hot and cold side, the following points were considered.

1. The channels containing hot fluid have a U-shaped cross-section such that the fillet radius, in comparison with its width and height, is negligible. Hence it is quite acceptable to be considered as a rectangle cross-section.
2. Due to its periodic configuration, just a section of whole channels has been modelled.
3. As this study is looking for the critical points, the selected section should be chosen from where there is highest temperature gradient, namely, the hot and cold entrances.
4. Gravity is dispensable and there is no heat generation
5. Air is considered as an incompressible Newtonian fluid and flow is in laminar regime

Governing Equation

For the thermo-hydrodynamic analysis of fluid flow and forced convection heat transfer through cross-flow plate heat exchanger, non-linear set of PDEs as the governing equations consist of conservation of mass, Eq. (9), momentum Eq. (10), and energy, Eq. (11), have to numerically be solved under certain boundary conditions and simplification assumptions.

$$\frac{\partial}{\partial x}(\rho u)+\frac{\partial}{\partial y}(\rho v)+\frac{\partial}{\partial z}(\rho w)=0 \quad (9)$$

$$\frac{\partial u_i}{\partial t}+u_j\frac{\partial u_i}{\partial x_i} = X_i - \frac{\partial p}{\partial x_i}+\nu\frac{\partial^2 u_i}{\partial x_j \partial x_i} \quad (10)$$

$$\frac{\partial}{\partial x}(\rho CuT - k_{th}\frac{\partial T}{\partial x})+\frac{\partial}{\partial y}(\rho CvT - k_{th}\frac{\partial T}{\partial y})+\frac{\partial}{\partial z}(\rho CwT - k_{th}\frac{\partial T}{\partial z}) = q'''_{gen} \quad (11)$$

Now to generalize the results to wide thermal geometrical conditions, by considering reference parameters for each variable, Eq. 12, governing equations turn into Non-dimensional form as follows:

$$x^* = \frac{x}{D_h},\ y^* = \frac{y}{D_h},\ z^* = \frac{z}{D_h},\ u^* = \frac{u}{\overline{V}},\ v^* = \frac{v}{\overline{V}},\ w^* = \frac{w}{\overline{V}},\ p^* = \frac{p}{\rho \overline{V}^2}$$
$$\mathrm{Re}_{ref} = \frac{\rho \overline{V} D_h}{\eta_{ref}},\ Pe = \frac{\overline{V} D_h}{\alpha},\ Ec = \frac{\overline{V}^2}{C_p \Delta T},\ T^* = \frac{T - T_{out}}{T_{in} - T_{out}} \quad (12)$$

$$\frac{\partial}{\partial x^*}(u^{*2} - \frac{1}{\mathrm{Re}}\frac{\partial u^*}{\partial x^*}) + \frac{\partial}{\partial y}(u^* v^* - \frac{1}{\mathrm{Re}}\frac{\partial u^*}{\partial y^*}) + \frac{\partial}{\partial z}(u^* w^* - \frac{1}{\mathrm{Re}}\frac{\partial u^*}{\partial z^*}) = -\frac{\partial p^*}{\partial x^*} \quad (13)$$

$$\frac{\partial}{\partial x^*}(u^* v^* - \frac{1}{\mathrm{Re}}\frac{\partial v^*}{\partial x^*}) + \frac{\partial}{\partial y^*}(v^{*2} - \frac{1}{\mathrm{Re}}\frac{\partial v^*}{\partial y^*}) + \frac{\partial}{\partial z^*}(v^* w^* - \frac{1}{\mathrm{Re}}\frac{\partial v^*}{\partial z^*}) = -\frac{\partial p^*}{\partial y^*} \quad (14)$$

$$\frac{\partial}{\partial x^*}(u^* w^* - \frac{1}{\mathrm{Re}}\frac{\partial w^*}{\partial x^*}) + \frac{\partial}{\partial y^*}(v^* w^* - \frac{1}{\mathrm{Re}}\frac{\partial w^*}{\partial y^*}) + \frac{\partial}{\partial z^*}(w^{*2} - \frac{1}{\mathrm{Re}}\frac{\partial w^*}{\partial z^*}) = -\frac{\partial p^*}{\partial z^*} \quad (15)$$

$$\frac{\partial}{\partial x^*}(u^* T^* - \frac{1}{Pe}\frac{\partial T^*}{\partial x^*}) + \frac{\partial}{\partial y^*}(v^* T^* - \frac{1}{Pe}\frac{\partial T^*}{\partial y^*}) + \frac{\partial}{\partial z}(w^* T^* - \frac{1}{Pe}\frac{\partial T^*}{\partial z^*}) = \frac{Ec}{\mathrm{Re}}\Phi^* \quad (16)$$

Where Φ is the dissipation energy loss due to viscous friction. The * value represented non-dimensional variable and hereafter, just for convenient, stars will be droped.

Assumptions and Boundary Conditions

To solve the governing equations of fluid flow motion and heat transfer these assumptions have been made.

1. Due to the fact that transient fluctuation attenuated rapidly through channels of small cross section area, and considering cruise speed for airplane, flows were considered in steady state.
2. The cold ambient air and the hot combustion product were considered Newtonian fluids
3. Fluid and solid materials were in thermally non-equilibrium conditions.

Computational Simulation

In "computation" step, Semi-Implicit Method for Pressure-Linked Equation (SIMPLE) of Patankar and Spalding was employed for introducing pressure into the continuity equation [20]. It is called semi- because the direct effect of pressure correction on velocity is dropped from the velocity correction equation, which causes very large pressure corrections. Also, the structured grid refined close to the boundary was generated and generalized Blocked-off region procedure was used to distinguish different zones (fluid or solid) for the code.

Moreover, finite difference forms of the partial differential equations (1) to (3) were obtained by integrating over an elemental cell volume with staggered control volumes for the r- and z-velocity components. Other variables of interest were computed at the grid nodes. Numerical solutions were obtained iteratively by the line-by-line method with progressing in the axial direction such that iterations were terminated when the sum of the relative residuals for all cells was less than specified small value for each equation.

Blocked-Off Method

To be able to adopt Cartesian coordinate system (CCS) for all type of geometries and avoid the complexity of treating non-orthogonal grids, it is appropriate to adopt a procedure to model complicated geometries using CCS. The blocked-off method includes drawing nominal domains around given physical domain, such that the whole region is divided into two parts: active and passive or blocked-off regions [21]. According to the blocked-off technique, known values of the dependent variables have to be established in all passive control volumes, Fig. 4. If the passive region represents a stationary solid boundary as in the case, the velocity components in that region must be equal to zero, and if the region is considered as an isothermal boundary, the known temperature have to be established in the passive control volumes. Correspondingly, when a radiant intensity enters, Lari and Gandjalikhan Nassab studied coupled radiative and conductive heat transfer problems in complex geometries with inhomogeneous and anisotropic scattering participating media in which, the blocked-off method was used for simulating the complex geometry [22].

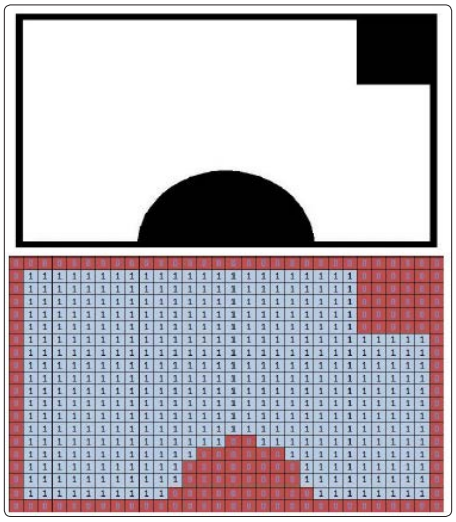

Figure 4: Schematic methodology of block-off for construction of complicated geometry in CCS

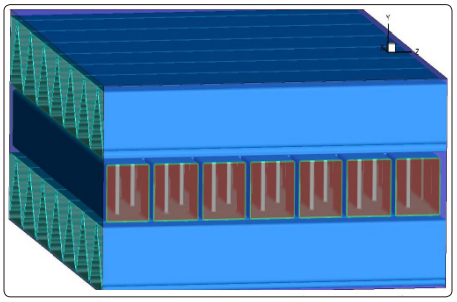

Figure 5: The complicated 3D geometry of plate cross-flow heat exchanger construction in Cartesian coordinate system, using block-off method.

According to the dimensions that have been already presented in Fig. 3, rectangular channels have a shift along its length at each 0.25-inch distance toward lateral direction. The flow directions in cross-flow heat exchanger are perpendicular to each other.

Grid generation and construction of precise model of complicated geometry for this plate heat exchanger in three-dimensional Cartesian coordinate system involves many complexities, Fig. 5. As an example, the thickness of plates is 0.005 in and height of channel is 0.125 in, which is 25 times bigger than plate thickness. While conduction heat transfer is going to solve through solid material, there have to be enough grid points such that numerical simulation could capture variations of dependent variable across computational domain. Structured mesh was designed such that at least 3 grid points fell across smallest dimension. At the same time, refining mesh to capture computational precision will increase total grid points and hence drastically increase computational time to run and converge. In Fig. 6, the generated mesh as well as a zoomed view of solid and fluid area gridlines is depicted.

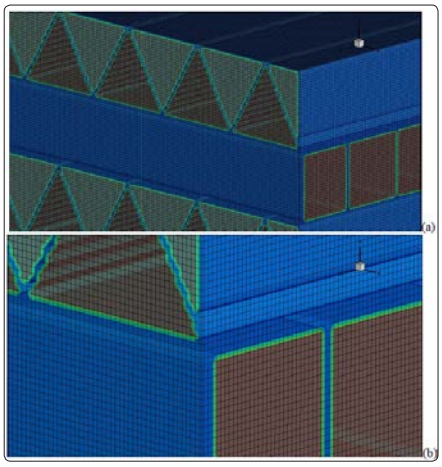

Figure 6: (a): Structured grid generation for 3D geometry of compact plate heat exchanger. (b): Zoomed view of cubic mesh

All numerical procedure is programmed in FORTRAN language which its arrangement is shown in Fig. 7, and architecture of connections of subroutines is displayed in Fig. 8. The numerical process begins with normalization of parameters to make all parameters non-dimensional, then grid generation with arithmetic method of clustering for the region adjacent to solid walls as well as high-gradient areas, was called. After that, geometry definition construct different part of heat exchanger such that solver can understand exactly the fluid and solid area.

The code is initialized with guess values, boundary conditions are set and iterative calculations starts for all nodes in computational domain and the values of pressure, temperature and velocity, in the three directions, are updated at each iteration. At the end of each iteration convergency is checked and, if the residuals of all governing equations go below a certain small value, then results will be saved and post processing prepares some files to display the numerical results.

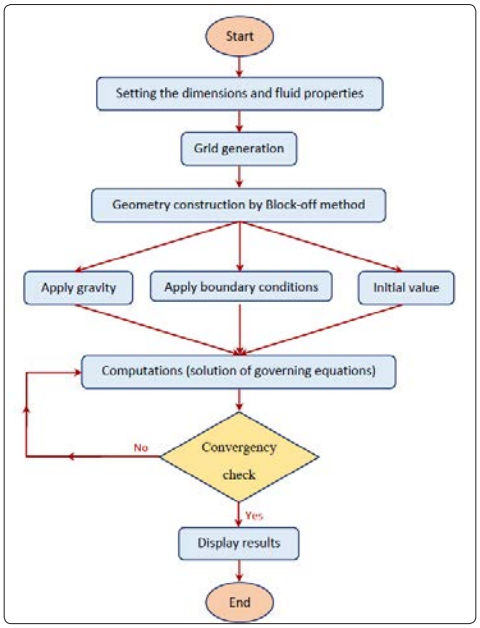

Figure 7: Flowchart of successive steps in the FORTRAN code

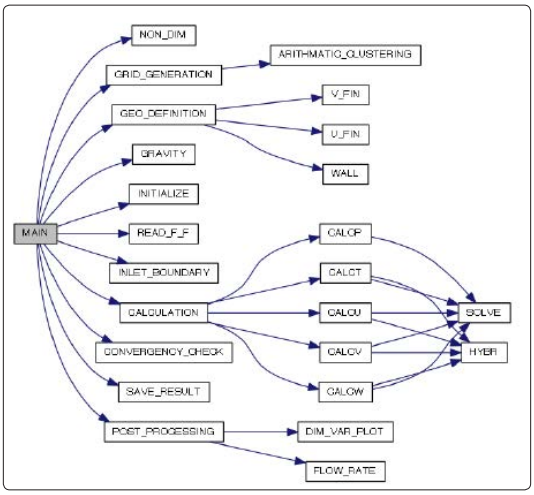

Figure 8: Structure of connections of subroutines in the FORTRAN code

Numerical Results and Discussion

As it is mentioned in numerical procedure, trend of variation of residual of momentum equation in the direction of hot and cold flows as well as continuity equation from the beginning to the convergency point is depicted in Fig. 9. The number of iterations was set such that the trend of residual of all equations becomes stable in a small value.

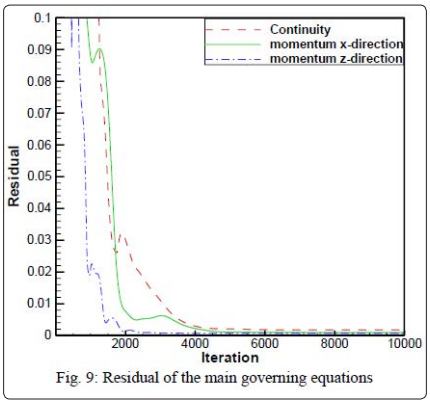

Figure 9: Residual of the main governing equations

Fig. 10 shows the evolution of velocity distribution from uniform flow at the entrance and its division at shifted walls along rectangular channels. In Fig. 10 (a), a y-plane cuts the geometry to show the variation of velocity distribution along the channel. Likewise, fig. 10 (b) and (c) were cited to show the velocity distribution in both cross-section area and longitudinal direction. The growth of boundary layer along the solid walls and the increase of velocity magnitude, when the cross-section area of channel decreased, can be tracked. The high-velocity flows from adjacent channel merged into a front single channel but due to the narrow low-velocity region at the channel centre, which is the extended path of stagnation point, there would be two maximum points for velocity profile instead of one. The velocity vector at the end of the channel also admits this fact.

Distribution of pressure along the rectangular channel is presented in Fig. 11 in which negative pressure gradient can obviously be seen. Moreover, at the stagnation point, where flow encounters the shifted wall along the hot channel and is divided into two branches,

due to the fact that dynamic pressure is added to the thermodynamic pressure, locally it occurs a small high-pressure region. In addition, while fluid flow over a blunt object, depending on its thickness, small low-pressure region occurs at a distance close to the stagnation point belongs to the small recirculation zone. It is good to notice that in the second shifted wall, when fluid flow hits the shifted plate, due to the phenomena mentioned above, due to the fact that maximum velocity does not happen at the centre of channel but instead there are two maximum shifted toward solid walls, the second stagnation point is not as significant as the first one.

In Fig. 12, the distribution of temperature profile across the hot and cold channel is depicted. This figure shows the evolution of temperature along rectangular and triangular channels where gradually forced convection along the hot side transfer heat flux to the cold side and becomes colder, while cold side absorbs this heat flux and becomes warmer. Moreover, high-temperature gradient occurs adjacent to the hot and cold entrances where cold air is at its lowest temperature and hot fluid is at its highest temperature. In fact, the physical phenomena as a reason behind the detachment problem of corrugated plates, that is the following: high temperature cause brazes to become soft and weak and, simultaneously, temperature gradient results in thermal stress and these two factors together lead to the plate detachment. This fact is also proved by the observation of heat exchanger, Fig. 13. As it is clearly seen, corruption and plate detachments mainly occur in the area already described.

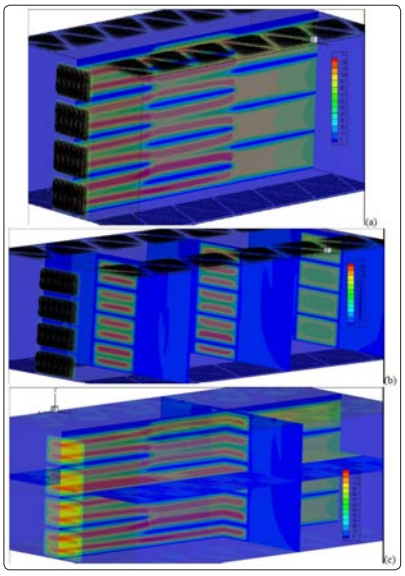

Figure 10: Velocity contour and vector, (a): Model is cut by the y-plane (b): Model is cut by the x-plane (c): Model is cut by the x-&y- planes

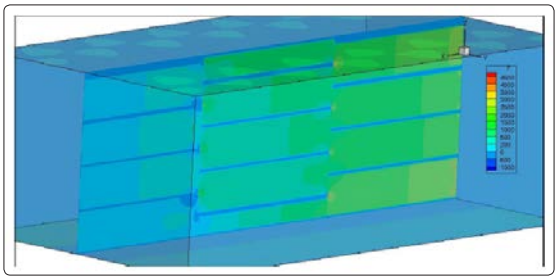

Figure 11: Pressure contour, y-plane cut along the rectangular channel

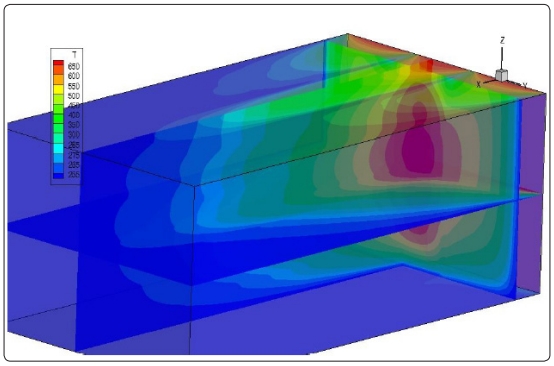

Figure 12: Contour of temperature across the hot channels

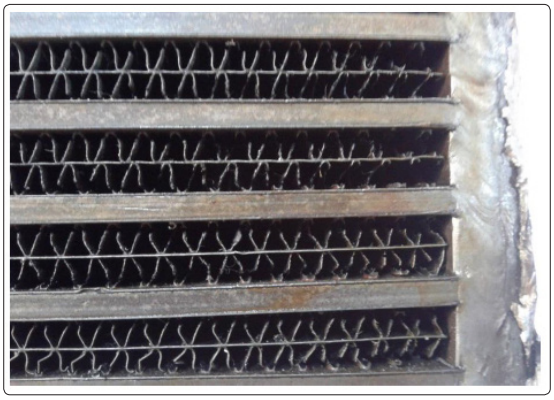

Figure 13: Corrupted detached plates adjacent to the entrance of heat exchanger

Conclusion

In this numerical study, three-dimensional thermo-hydrodynamic analysis of air-to-air cross-flow plate heat exchanger for steady state laminar flow of single-phase Newtonian fluid with constant property is investigated. The conjugate heat transfer consists of forced convection for fluid flow and conduction through solid part were considered. The set of non-linear PDE as the governing equations were discredited by FVM and numerically solved by the SIMPLE algorithm. The liberalized set of equations was iteratively solved by TDMA method, such that the convergence occurs when residual of all governing equation reaches to a small value. It is important to remind that the problem of corrugated plate detachment occurs under the presence of both high temperatures to make brazes weak and high-temperature gradient to have enough strong thermal force to detach the plates. According to the temperature distribution, this situation happens at the entrance of cold/hot channels that are adjacent to hot/cold walls. Another critical area is the first leading edge of displaced rectangular channels that are on the way of hot fluid. Due to the high dynamic pressure accompanied by high temperature that occurs in this area, detachment problem is likely to happen. Suggested solutions for this problem are as follows:

1. Using brazes with higher thermal resistance only for critical areas specified in this work, which are not a lot, will highly reduce the occurrence of this problem.
2. According to the temperature distribution, it is found that displaced rectangular channel from hot side did not lead to a thermal gain. If they were constructed monolithic, with no displacement along the channels then, at least, it has more mechanical strength.

3. While there is a pressure loss along the channel, the difference between pressure of hot and cold side at the end of channel is much less than its value at the beginning of the channel. It implies that if we change the inlet and outlet of hot side, such that corrupted part fells at the end of the channel, we could reuse the heat exchanger with much less leakage.

Acknowledgement

Acknowledgement to the research unit integrated projects UID/EMS/00481/2013-FCT and CENTRO-01-0145-FEDER-022083

References

1. Sheikhnejad Y, Hosseini R, Saffar Avval M (2017) Experimental study on heat transfer enhancement of laminar ferrofluid flow in horizontal tube partially filled porous media under fixed parallel magnet bars. J of Magnetism and Magnetic Materials 424: 16-25.
2. Sheikhnejad Y, Hosseini MM, Shahpari A, Teixeira A, Hosseini R et al., (2017) Experimental Investigation and Three Dimensional Numerical Analysis of Ferroconvection Through Horizontal Tube Under Magnetic Field of Fixed Parallel Magnet Bars. ASME J Heat Transfer.
3. Sheikhnejad Y, Hosseini R, Saffar-avval M (2015) Laminar forced convection of ferrofluid in a horizontal tube partially field with porous media in the presence of magnetic field. J Porous Media 18: 437-448.
4. Sheikhnejad Y, Hosseini R, Saffar Avval M (2015) Effect of different magnetic field distributions on laminar ferroconvection heat transfer in horizontal tube. Journal of Magnetism and Magnetic Materials 389: 136-143.
5. Maghsoudi P, Sadeghi S, Hanafizadeh P (2017) Thermo economic optimization of plate-fin heat exchanger using louver off-set strip, triangular and rectangular fins applied in 200 kW microturbines. ASME J Heat Transfer.
6. Nilpueng K, Keawkamrop T, Ahn HS, Wongwises S (2018) Effect of chevron angle and surface roughness on thermal performance of single-phase water flow inside a plate heat exchanger. International Communications in Heat and Mass Transfer 91: 201-209.
7. Bhattad A, Sarkar J, Ghosh P (2018) Discrete phase numerical model and experimental study of hybrid nanofluid heat transfer and pressure drop in plate heat exchanger. International Communications in Heat and Mass Transfer 91: 262-273.
8. Gwo-Geng Lin, Chii-Dong Ho, Jung-Jeng Huang, Yu-Ru (2012) Chen Heat transfer enhancement for the power-law fluids through a parallel-plate double-pass heat exchangers with external recycle. International Communications in Heat and Mass Transfer 39: 1111-1118.
9. Khoshvaght-Aliabadi M, Jafari A, Sartipzadeh O, Salami M (2016) Thermal–hydraulic performance of wavy plate-fin heat exchanger using passive techniques: Perforations, winglets, and nanofluids. International Communications in Heat and Mass Transfer 78: 231-240.
10. Moslem Yousefi, Rasul Enayatifar, Amer Nordin Darus, Abdul Hanan Abdullah (2012) A robust learning based evolutionary approach for thermal-economic optimization of compact heat exchangers. International Communications in Heat and Mass Transfer 39: 1605-1615.
11. Khairul MA, Alim MA, Mahbubul IM, Saidur R, Hepbasli A (2014) Heat transfer performance and energy analyses of a corrugated plate heat exchanger using metal oxide nano fluids. International Communications in Heat and Mass Transfer 50: 8-14.
12. Javadi FS, Sadeghipour S, Saidur R, BoroumandJazi G, Rahmati B et al., (2013) The effects of nanofluid on thermophysical properties and heat transfer characteristics of a plate heat exchanger. International Communications in Heat and Mass Transfer 44: 58-63.
13. Sheik Ismail L, Velraj R (2009) Studies on Fanning Friction (f) and Colburn (j) Factors of Offset and Wavy Fins Compact Plate Fin Heat Exchanger–A CFD Approach. Numerical Heat Transfer Part a 56: 987-1005.
14. Li-Zhi Zhang (2007) thermally developing forced convection and heat transfer in rectangular plate-fin passages under uniform plate temperature. Numerical Heat Transfer Part A 52: 549-564.
15. Luan HB, Kuang JP, Cao Z, Wu Z, Tao WQ (2017) CFD analysis of two types of welded plate heat exchangers. Numerical Heat Transfer part A 71: 250-269.
16. Geometric altitude vs. temperature, pressure, density, and the speed of sound derived from the 1962 U.S. Standard Atmosphere.
17. U.S. Standard Atmosphere, U.S. Government Printing Office, Washington, D.C., 1976.
18. U.S. Extension to the ICAO Standard Atmosphere, U.S. Government Printing Office, Washington, D.C., 1958.
19. F. M. White (1991) Viscos fluid flow, 2nd edition, McGraw-Hill Inc.
20. Ansari AB, Gandjalikhan Nassab SA (2013) Forced Convection of Radiating Gas over an inclined backward facing step using the blocked-off methods. J of Thermal Science 17: 773-786.
21. Lari K, Gandjalikhan Nassab SA (2012) Modeling of the Conjugate Radiation and Conduction Problem in a 3-D Complex Multi-Burner Furnace Thermal Science 16: 1187-1200.
22. Patankar SV (1980) Numerical heat transfer and fluid flow, McGRAW-HILL Book Company, Hemisphere Publication Corporation.